Hindawi
Mathematical Problems in Engineering
Volume 2021, Article ID 6649454, 7 pages
https://doi.org/10.1155/2021/6649454

Research Article

Ant Colony Optimization Inversion Using the L1 Norm in Advanced Tunnel Detection

Zhao Ma,[1,2] **Lichao Nie**,[1,3] **Pengfei Zhou**,[4] **Zhaoyang Deng**,[1,3] **and Lei Guo**[5]

[1]*Geotechnical and Structural Engineering Research Center, Shandong University, Jinan 250061, China*
[2]*School of Qilu Transportation, Shandong University, Jinan 250061, China*
[3]*School of Civil Engineering, Shandong University, Jinan 250061, China*
[4]*Qilu Transportation Development Group Co., LTD, Jinan, Shandong 250101, China*
[5]*Shandong Provincial Communications Planning and Design Institute Co., LTD, Jinan, Shandong 250101, China*

Correspondence should be addressed to Lichao Nie; lichaonie@163.com

Received 27 December 2020; Revised 12 March 2021; Accepted 1 April 2021; Published 13 April 2021

Academic Editor: Thomas Hanne

During the construction of the tunnel, there may be water-bearing anomalous structures such as fault fracture zone. In order to ensure the safety of the tunnel, it is necessary to carry out advanced tunnel detection. The traditional linear inversion method is highly dependent on the initial model in the tunnel resistivity inversion, which makes the inversion results falling into the local optimal optimum rather than the global one. Therefore, an inversion method for tunnel resistivity advanced detection based on ant colony algorithm is proposed in this paper. In order to improve the accuracy of tunnel advanced detection of deep anomalous bodies, an ant colony optimization (ACO) inversion is used by integrating depth weighting into the inversion function. At the same time, in view of the high efficiency and low cost of one-dimension inversion and the advantages of L1 norm in boundary characterization, a one-dimensional ant colony algorithm is adopted in this paper. In order to evaluate the performance of the algorithm, two sets of numerical simulations were carried out. Finally, the application of the actual tunnel water-bearing anomalous structure was carried out in a real example to evaluate the application effect, and it was verified by excavation exposure.

1. Introduction

Geophysical inversion is an effective method to find a model with a response similar to the actual measured values. All inversion methods are essential to determine the underground model whose response is consistent with the measured data within certain restrictions and acceptable limits [1]. For example, Liu et al. [2] performed linear inversion by using the least-square 4D resistivity inversion method, which can quickly locate and depict the change in resistivity with high accuracy. In addition, one commonly used version of the geophysical inversion is nonlinear inversion which is widely used in various fields. For example, deep leaning algorithm of the nonlinear inversion method has been applied to the resistivity and seismic fields and achieved good results [3, 4]. Song et al. [5] proposed a novel multipopulation parallel co-evolutionary differential evolution, which can achieve superior performance on the accuracy, stability, and robustness. Deng et al. [6] proposed a novel improved differential evolution algorithm and a new optimal mutation strategy based on the wavelet basis function. It can improve the search quality, accelerate convergence, and avoid falling into local optimum and stagnation. Song et al. [7] proposed a parameter optimization method based on enhanced success history adaptive differential evolution algorithm with greedy mutation strategy. Deng et al. [8] presented an improved quantum evolutionary algorithm based on the niche co-evolution strategy and enhanced particle swarm optimization, which can achieve better results on optimization performance, robustness, and stability. An enhanced improved quantum-inspired differential evolution with multistrategies was proposed by Deng et al. [9], which can improve search accuracy, accelerate convergence, and achieve the optimal solution.

In particular, great progress has been made in non linear inversion methods in the field of tunnel detection. For example, Nguyen et al. [10] proposed a new hybridized global optimization method combining simulated annealing global search with the minimization of trackless Kalman filtering, which was used to solve the waveform inversion problem of advanced prediction of the underground tunnel face. The particle swarm optimization and homotopy optimization were applied to the displacement back analysis in tunnel engineering by Hu et al.[11]. Park et al. [12, 13] used the harmony search method to predict the location, permittivity ratio, and conductivity of the anomalous zone of a tunnel face by utilizing the electrical resistivity of the ground. Nie et al. [14] provide a joint inversion method based on an ant colony algorithm and least-square inversion method, which could present a better identification of the position and spatial shape of the water-bearing structure in the tunnel ahead prospecting.

Ant colony optimization was introduced in the early 1990s by Marco Dorigo and colleagues [15, 16]. The ACO algorithm is inspired by the ants' foraging behavior. The core of this behavior is the indirect communication between ants via the chemical pheromone trails, which allow them to find shortcuts between the nest and a food source through their cooperation. ACO algorithm has been widely used in optimization problems, which has advantages of positive feedback, parallelism, and robustness [17]. Since the observed data generated by different electrode intervals is related to the buried depth [18], the data weighting factor is introduced into the ACO to optimize the algorithm. In this case, the ACO algorithm based on data weighting is proposed in this paper.

The common approach in the regularization optimization method is the smoothness-constrained or L2 norm method [19]. Under the condition of stable underground geological changes, the model recovered by the L2 norm method has typical smooth characteristics and will give positive results [20]. However, in regions of sharp transition in the subsurface resistivity, this method usually cannot reconstruct these sharp geological changes well [21]. In contrast, the L1 norm tends to generate piecewise continuous models and produce models separated by sharp boundaries [22]. This might be more consistent with the complex environment of the tunnel, such as the presence of fault fracture zones ahead of the tunnel face utilizing electrical resistivity.

The rest of the article is arranged as follows. We first briefly introduce the ACO inversion with L1 norm or L2 norm. We also describe the procedures for ACO inversion in advanced tunnel detection. We illustrate the effectiveness of this inversion method by applying it to synthetic examples and field survey in a tunnel environment. The field data were collected from the water conveyance project from Songhua River in the middle of Jilin province.

2. Methodology

2.1. The Ant Colony Optimization. The ant colony algorithm is a method that ants find the shortest path from their nest to a food source. The core of this behavior is the indirect communication between ants through chemical pheromone trails. When the ants are looking for food, they will initially explore the area around the nest in a random manner. During exploring, ants will leave chemical pheromone on the ground. Once an ant finds a food source, it evaluates the quantity and quality of the food and brings some back to the nest. The amount of pheromones ants left on the ground during the return depends on the quantity and quality of food. Pheromone will guide other ants to find a food source [23]. The main parameters are described below.

The objective function of resistivity inversion based on the *Lp* norm ACO algorithm is as follows:

$$\Phi_{mn} = \sum_{i=1}^{N} \left| \frac{\rho_{di} - \rho_{si}}{\rho_{di}} \right|^{p}, \quad p = 1, 2, \tag{1}$$

where Φ_{mn} is the data constraints, N represents the number of observed data, and ρ_{di} and ρ_{si} represent the ith observed data and predicted data, respectively. The objective function expression is expressed as the L1 norm when $p = 1$, otherwise it is L2 norm. In order to better use the resistivity method to detect the water-bearing fault zone ahead of the tunnel face, the L1 norm is adopted, *i.e.*, $p = 1$. When Φ_{mn} reaches the global minimum, the foraging path chosen by ants is the shortest. The model parameters corresponding to the shortest path are the inversion results.

As the electrode spacing increases, the sensitivity of the observed data to the deep also increases. The data weighting factor is introduced into the inversion problem to increase the weight of effective observed data. Therefore, the objective function of the ACO algorithm based on the L1 norm is expressed as follows [18, 24, 25]:

$$\Phi_{mn} = \sum_{i=1}^{N} \left| w_i \frac{\rho_{di} - \rho_{si}}{\rho_{di}} \right|^{1},$$
$$w_i = k_0 z_i + z_0, \tag{2}$$

where w_i represents the data weighting factor, k_0 and z_0 are constants, and z_i is the distance between tunnel face and current electrode of the ith circle along z direction.

The probability of ants transferring from one cell to another is determined by pheromone intensity and visibility. The transition probability is expressed as follows [26]:

$$P_{ij}^{k} = \frac{\left[\tau_{ij}\right]^{\alpha} \cdot \left[\eta_{ij}\right]^{\beta}}{\sum_{i=1}^{\text{num}} \left[\tau_{ij}\right]^{\alpha} \cdot \left[\eta_{ij}\right]^{\beta}}, \tag{3}$$

where P_{ij}^{k} represents stochastically tour from node j is selected by ant k to be visited after node i, τ_{ij} is the pheromone intensity on the jth node of the ith cell, η_{ij} is visibility about the path that ant transited from the ith node to jth node, and α and β are weight factors of pheromone intensity and visibility, respectively. In order to calculate the visibility of the path, it can be expressed as

$$\eta_{ij} = \frac{1}{\left|\rho_{i-1j-1} - \rho_{ij}\right| + \rho_0}, \tag{4}$$

where ρ_{ij} represents the resistivity value of the jth node selected on the ith cell and ρ_0 is half of the resistivity range of the ith cell. It can be shown that the smaller the difference between two cells, the larger the transition probability.

At the beginning, k ants were randomly placed. Then, each ant decides the next node to visit according to the P_{ij}^k given by Equation (3). After iterating this process t times, each ant completes a tour. When ants are passing through the path, they generate new pheromone, and the intensity of the original pheromone would evaporate over time. Obviously, ants with the shorter tours will leave more pheromones than ants with the longer tours. Furthermore, when a group of ants passes this path, the pheromone will be updated. Therefore, the pheromone is updated as follows [23, 27]:

$$\tau_{ij}^{\text{new}} = \lambda \tau_{ij}^{\text{old}} + \Delta\tau_{ij}^{k},$$

$$\Delta\tau_{ij}^{k} = \begin{cases} \dfrac{Q}{\phi_{mn}}, & \text{if ant k pass through the node } (i, j), \\ 0, & \text{otherwise,} \end{cases} \quad (5)$$

where τ_{ij}^{new} represents the intensity after pheromone update, τ_{ij}^{old} represents the intensity of the original pheromone, $\lambda \in (0, 1)$ is the volatility coefficient of pheromone trails, which avoids the infinite accumulation of pheromones, and Q is the total quantity of pheromone.

To solve the problem of normal L1 norm inversion, the main methods include the iterative shrinkage thresholding/shaping method [28–30], the preconditioned conjugate gradient (PCG) method [31, 32], and split-Bregman method [33]. Among them, the PCG method has the advantages of solving the convenient inverse matrix and accelerating the convergence rate [34]. Therefore, the PCG method is used to solve the inversion problem in this paper.

2.2. Process of Ant Colony Optimization Inversion for Tunnel Detection. First, the 3D induced polarization method was used for forward modeling of advanced detection in tunnel [35]. The potential electrode M placed on the tunnel face and the current electrodes A1~A4 are arranged on the tunnel outline, as shown in Figure 1. During the tunnel detection process, the four current electrodes on the tunnel surface are injected with the current at first. The potential electrodes on the tunnel face collect observed data, and then, the current electrode ring is moved away from the tunnel face and the current is injected again. Repeating this operation, the distance between the current electrode A and the potential electrode M gradually increases. The current electrode B and potential electrode N are arranged at a remote distance from the tunnel face.

For 3D resistivity forward tunnel modeling problems, the finite element method is used in this paper. In particular, as for the model grid division, the inversion area in front of the tunnel is divided into 10 layers, and each layer is 3 m.

Finally, the ACO algorithm for inversion is used, and the process is as follows:

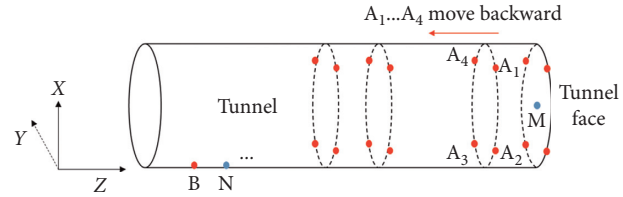

Figure 1: Schematic diagram for induced polarization advanced prediction in the tunnel. The position of electrodes B and N are at a remote distance from tunnel face.

(1) Initializing the parameters: input number of a group ant, upper limits of iteration, and other parameters.

(2) Ants choose paths based on the transition probability P_{ij}^k.

(3) Calculate objective function value Φ_{mn} for each ant, and select a global minimum model parameter up to now.

(4) Update pheromone intensity $\Delta\tau_{ij}^k$ and execute the next iteration. If the objective function Φ_{mn} bellows the tolerance ψ or the iteration times exceed the upper limits N_i, the final result will be outputted.

2.3. Numerical Simulation. To illustrate the efficiency of the ACO algorithm based on the L1 norm in the 1D layered stratum inversion of the tunnel, the algorithm was tested using two synthetic examples to simulate the water-bearing fault.

The first model example is shown in Figure 2(a). The size of the tunnel face was used is $8\,m \times 8$ m. According to the calculation experience, the value of k_0 and z_0 are both 1 in the L1 norm and 1.8 and 1 in the L2 norm, respectively. An anomalous layer is located 12 m ahead of the tunnel face, and its thickness is 3 m. The background resistivity of the model is 1000 Ωm, and the anomalous layer with a resistivity of 400 Ωm.

Figures 2(b) and 2(c), respectively, show the inverted 1D geoelectrical models. Results are obtained using the L1 norm and L2 norm ACO. One can see that the location of the anomalous layer was reconstructed very well, and the depth from the tunnel face is about 12 m, which is consistent with the real distance. The resistivity of the anomalous in Figure 2(b) is about 530 Ωm, which is not much different from the real resistivity value. Comparing with the result of the L1 norm, the location of the low resistivity area is about 12 m and the resistivity is about 830 Ωm in Figure 2(c), but it is not reflecting the resistivity of the anomalous layer well.

The second model consists of one anomalous layer with a low resistivity value (400 Ωm), which is located at 21 m along z-axis. Other parameters' settings are shown in model 1. As a result, the location of the low resistivity layer is about 21 m along z-axis, and the resistivity is about 420 Ωm in Figure 2(e); the position and region of the anomalous body are consistent with the actual one. In contrast, the result of the L2 norm deviates from the actual mode more than the result of the L1 norm. The position of the low resistivity

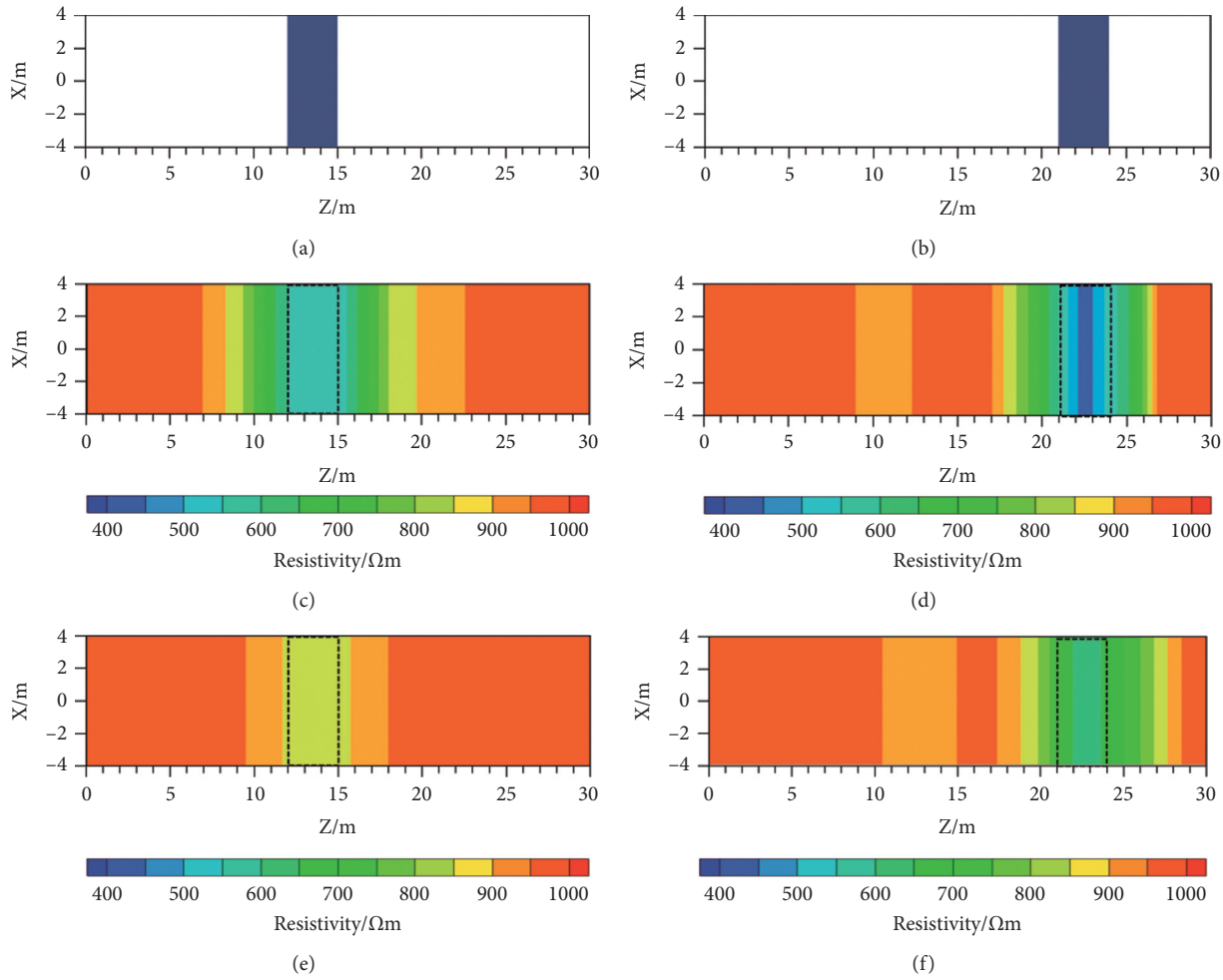

Figure 2: Inversion results for two models with low resistivity. (a) True resistivity of model 1. The results obtained after inversion of model 1 are shown in (b) using L1 norm and (c) using L2 norm. (d) Sketch of model 2. The results obtained after inversion of model 2 are shown in (e) using L1 norm and (f) using L2 norm. The black dotted frame represents the actual location of the low resistivity layer set by the model.

anomalous is about 22 m along the z-axis, and the resistivity value is about 590 Ωm.

From the two numerical simulations, the inversion results show that the L1 norm is more effective than the L2 norm in reflecting the position and resistivity of the low resistivity layer ahead of the tunnel face. These results will be verified in the field data.

2.4. Application Example. To examine the efficiency of the inversion algorithm on the tunnel detection, we inverted 1D resistivity data from the water conveyance project from Songhua River in the middle of Jilin province. The No.4 contract section of the main line construction is located between the Chalu River and Yinma River sections in Jilin City, the survey area at the tunnel mileage of 64 + 728 – 64 + 698 m. According to the geological reconnaissance, the surrounding rock in this section is mainly limestone, and the integrity of the rock mass is poor. Moreover, this section is with the scope of the fault.

We adopted the induced polarization method proposed by Li et al. [16] to collect and process data. The inversion results of the L1 norm and L2 norm are illustrated by using the 1D ACO and are shown in Figure 3. The inversion grid division is consistent with numerical simulation. The number of iterations reached 20 when calculating the cut-off conditions. From Figure 3(a), it can be seen that the region of the low resistivity anomalous body is approximately from 0 m to 10 m, and the value of resistivity is approximately below 500 Ωm. Figure 3(b) shows the result of the observed data using the L2 norm. It can be observed that the low resistivity area is approximately 2 m to 14 m along the z-axis. The color of the low resistivity area is lighter than that of Figure 3(a), which means that its value is relatively high, around 500–600 Ωm.

According to the tunneling exposures shown in Figure 4, tunnel exaction encountered water gushing at 64 + 728 m to 64 + 718 m. The influence range of the water body is 0 m to 10 m ahead tunnel face. It was revealed by field excavation, as shown in Figure 5, that the water inflow is 1500 m^3 per hour at 64 + 727. The excavation result is consistent with the result

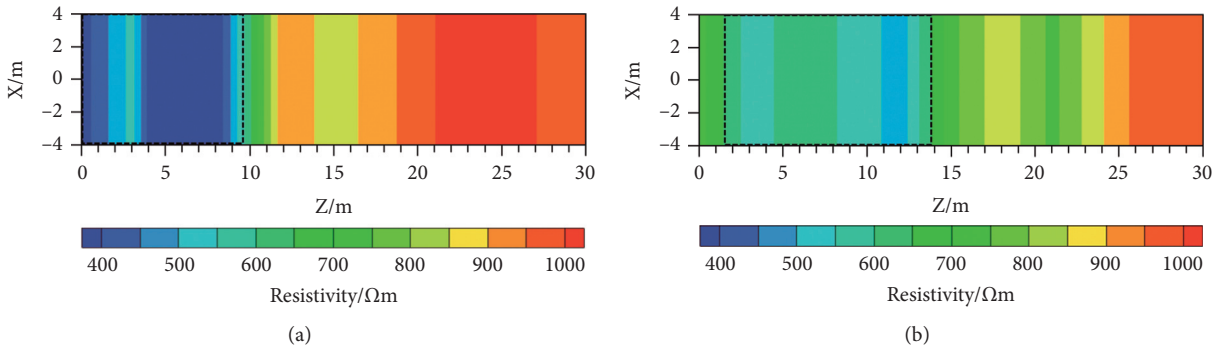

Figure 3: Inversion results for field data. (a) L1 norm inversion imaging. (b) L2 norm inversion imaging. The black dotted frame represents the low resistivity anomalous body.

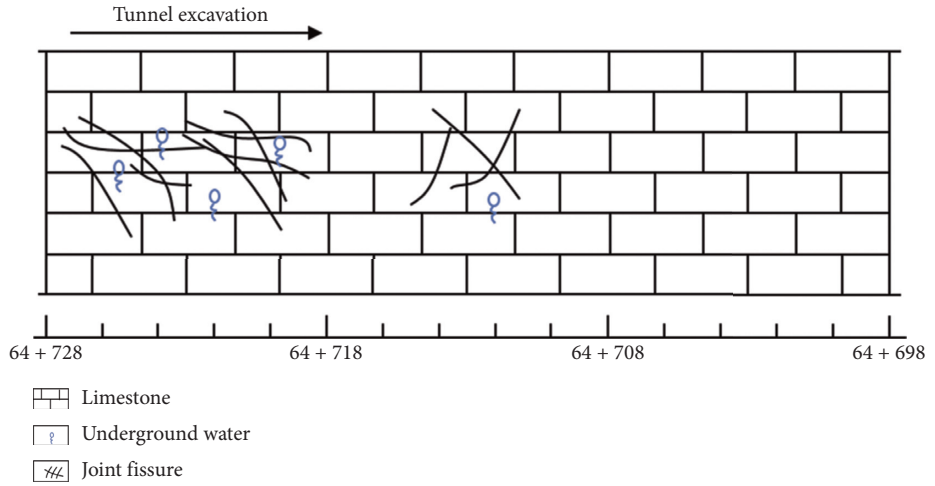

Figure 4: The complete section projection drawing of the geologic sketch and the excavation mileage is from 64 + 728 m to 64 + 698 m.

Figure 5: The excavation results at 64 + 727.

obtained by L1 norm inversion. On the whole, the ACO inversion algorithm based on the L1 norm could better estimate the low resistivity anomalous bodies than the L2 norm.

3. Conclusions

In this paper, an ACO algorithm based on the L1 norm is proposed for advanced tunnel detection. The key component of this approach is using the 3D induced polarization method to collect and process the data in the forward modeling. The inversion adopts the data weighting L1 norm ACO, which can increase the weight of effective data in the deep, so as to locate the deep anomalous bodies.

The proposed method provides an ACO algorithm using the L1 norm for tunnel advance detection. Compared to the L2 norm method, the developed method produces a better effect in identifying the sharp boundary of low resistivity anomalous bodies.

The developed method was tested using the two low resistivity models to simulate the water-bearing fault, and the 1D distribution of low resistivity body can be recovered by this inversion method. The method was applied to the field detection of the water conveyance project from Songhua River in the middle of Jilin province, which was verified through tunnel excavation.

Data Availability

The data used to support the findings of the study are available from the corresponding author upon request.

Conflicts of Interest

The authors declare that there are no conflicts of interest regarding the publication of this paper.

Acknowledgments

This work was supported by the Science & Technology Program of Department of Transport of Shandong Province under Grant no. 2019B47_2.

References

[1] M. H. Loke, Tutorial: 2-D and 3-D electrical imaging surveys, 2004, https://www.geotomosoft.com/coursenotes.zip.

[2] B. Liu, Y. Pang, D. Mao et al., "A rapid four-dimensional resistivity data inversion method using temporal segmentation," *Geophysical Journal International*, vol. 221, no. 1, pp. 586–602, 2020.

[3] B. Liu, Q. Guo, S. C. Li et al., "Deep learning inversion of electrical resistivity data," *IEEE Transactions on Geoscience and Remote Sensing*, vol. 58, no. 8, pp. 5715–5728.

[4] S. Li, B. Liu, Y. Ren et al., "Deep-learning inversion of seismic data," *IEEE Transactions on Geoscience and Remote Sensing*, vol. 58, no. 3, pp. 2135–2149, 2020.

[5] Y. J. Song, D. Q. Wu, W. Deng et al., "Multi-population parallel co-evolutionary differential evolution for parameter optimization," *Energy Conversion and Management*, vol. 228, 2021.

[6] W. Deng, J. J. Xu, Y. J. Song, and H. M. Zhao, "Differential evolution algorithm with wavelet basis function and optimal mutation strategy for complex optimization problem," *Applied Soft Computing*, vol. 100, 2020.

[7] Y. J. Song, D. Q. Wu, A. W. Mohamed, X. B. Zhou, B. Zhang, and W. Deng, "Enhanced success history adaptive DE for parameter optimization of photovoltaic models," *Complexity*, vol. 2021, Article ID 6660115, 22 pages, 2021.

[8] W. Deng, J. J. Xu, H. M. Zhao, and Y. J. Song, "A novel gate resource allocation method using improved PSO-based QEA," *IEEE Transactions on Intelligent Transportation Systems*, vol. 99, 2020.

[9] W. Deng, J. J. Xu, X. Z. Gao, and H. M. Zhao, "An enhanced MSIQDE algorithm with novel multiple strategies for global optimization problems," *IEEE Transactions on Systems, Man, and Cybernetics: Systems*, vol. 99, 2020.

[10] L. T. Nguyen and T. Nestorović, "Unscented hybrid simulated annealing for fast inversion of tunnel seismic waves," *Computer Methods in Applied Mechanics and Engineering*, vol. 301, pp. 281–299, 2016.

[11] J. P. Hu, Y. L. Liu, X. He, and J. H. Wen, "A novel hybrid algorithm with marriage of particle swarm optimization and homotopy optimization for tunnel parameter inversion," *Applied Mechanics and Materials*, vol. 231, pp. 2033–2037, 2012.

[12] J. Park, K.-H. Lee, J. Park, H. Choi, and I.-M. Lee, "Predicting anomalous zone ahead of tunnel face utilizing electrical resistivity: I. Algorithm and measuring system development," *Tunnelling and Underground Space Technology*, vol. 60, pp. 141–150, 2016.

[13] J. Park, K.-H. Lee, B.-K. Kim, H. Choi, and I.-M. Lee, "Predicting anomalous zone ahead of tunnel face utilizing electrical resistivity: II. Field tests," *Tunnelling and Underground Space Technology*, vol. 68, pp. 1–10, 2017.

[14] L. C. Nie, X. X. Zhang, B. Liu et al., "A study on resistivity imaging in tunnel ahead prospecting based on GPU joint inversion," *Chinese Journal of Geophysics*, vol. 82, 2017.

[15] M. Dorigo, V. Maniezzo, and A. Colorni, "Ant System: optimization by a colony of cooperating agents," *IEEE Trans Syst Man Cybernet Part B*, vol. 26, no. 1, pp. 1–13, 1996.

[16] C. Blum, "Ant colony optimization introduction and recent," *Physics of Life Reviews*, vol. 2, no. 4, 2006.

[17] C. R. Conti, M. Roisenberg, G. Neto, and M. J. Porsani, "Fast seismic inversion methods using ant colony optimization algorithm," *IEEE Geoscience and Remote Sensing Letters*, vol. 10, no. 5, pp. 1119–1123, 2013.

[18] L. Nie, Z. Ma, B. Liu et al., "A weighting function-based method for resistivity inversion in subsurface investigations," *Journal of Environmental and Engineering Geophysics*, vol. 25, no. 1, pp. 129–138, 2020.

[19] C. deGroot-Hedlin and S. Constable, "Occam's inversion to generate smooth, two-dimensional models from magnetotelluric data," *Geophysics*, vol. 55, pp. 1613–1624, 1990.

[20] C. G. Farquharson, "Constructing piecewise-constant models in multidimensional minimum-structure inversions"" *Geophysics*, vol. 73, 2008.

[21] J. Sun and Y. Li, "Adaptive Lp inversion for simultaneous recovery of both blocky and smooth features in a geophysical model," *Geophysical Journal International*, vol. 197, no. 2, pp. 882–899, 2014.

[22] M. H. Loke, I. Acworth, and T. Dahlin, "A comparison of smooth and blocky inversion methods in 2D electrical imaging surveys," *Exploration Geophysics*, vol. 34, no. 3, pp. 182–187, 2003.

[23] C. Blum, "Ant colony optimization: introduction and recent trends," *Physics of Life Reviews*, vol. 2, no. 4, pp. 353–373, 2005.

[24] C. G. Farquharson and D. W. Oldenburg, "Non-linear inversion using general measures of data misfit and model structure," *Geophysical Journal International*, vol. 134, no. 1, pp. 213–227, 1998.

[25] L.-Y. Zhang and H.-F. Liu, "The application of ABP method in high-density resistivity method inversion," *Chinese Journal of Geophysics*, vol. 54, no. 1, pp. 64–71, 2011.

[26] L. Huang, C. Zhou, and K. Wang, "Hybrid ant colony algorithm for traveling salesman problem," *Progress in Natural Science*, vol. 13, no. 4, pp. 295–299, 2003.

[27] S. Liu, X. Hu, and T. Liu, "A stochastic inversion method for potential field data: ant colony optimization," *Pure and Applied Geophysics*, vol. 171, no. 7, pp. 1531–1555, 2014.

[28] Y. Chen, S. Fomel, and J. Hu, "Iterative deblending of simultaneous-source seismic data using seislet-domain shaping regularization," *Geophysics*, vol. 79, no. 5, pp. V179–V189, 2014.

[29] S. Gan, S. Wang, Y. Chen, X. Chen, W. Huang, and H. Chen, "Compressive sensing for seismic data reconstruction via fast projection onto convex sets based on seislet transform," *Journal of Applied Geophysics*, vol. 130, pp. 194–208, 2016.

[30] S. Zu, H. Zhou, W. Mao et al., "Iterative deblending of simultaneous-source data using a coherency-pass shaping operator," *Geophysical Journal International*, vol. 211, no. 1, pp. 541–557, 2017.

[31] Y. K. Chen, "Automatic Velocity Analysis Using High-Resolution Hyperbolic Radon transformAutomatic Velocity Analysis," *Geophysics*, vol. 83, 2018.

[32] H. Wang, G. T. Huang, W. Chen, and Y. K. Chen, "Q-compensated denoising of seismic data," *IEEE Transactions on Geoscience and Remote Sensing*, vol. 59, no. 4, pp. 3580–3587, 2021.

[33] S. Qu, E. Verschuur, and Y. K. Chen, "Full waveform inversion and joint migration inversion with an automatic directional total variation constraint," *Geophysics*, vol. 84, pp. 1–37, 2019.

[34] B. Liu, S. C. Li, L. C. Nie, J. Wang, and Q. S. Zhang, "3D resistivity inversion using an improved Genetic Algorithm based on control method of mutation direction," *Journal of Applied Geophysics*, vol. 87, pp. 1–8, 2012.

[35] S. Li, L. Nie, and B. Liu, "The practice of forward prospecting of adverse geology applied to hard rock TBM tunnel construction: the case of the Songhua River water conveyance project in the middle of Jilin province," *Engineering*, vol. 4, no. 1, pp. 131–137, 2018.